

# Ultrafast Energy Transfer in Binuclear Ruthenium–Osmium Complexes as Models for Light-harvesting Antennas

Helena Berglund Baudin,<sup>†</sup> Jan Davidsson,<sup>†</sup> Scolastica Serroni,<sup>‡</sup> Alberto Juris,<sup>§</sup>  
Vincenzo Balzani,<sup>§</sup> Sebastiano Campagna,<sup>‡</sup> and Leif Hammarström<sup>\*,†</sup>

Department of Physical Chemistry, Uppsala University, Box 532, S-751 21 Uppsala, Sweden, Dipartimento di Chimica Inorganica, Chimica Analitica e Chimica Fisica, Università di Messina, via Sperone 31, 98166 Messina, Italy, and Dipartimento di Chimica "G. Ciamician", Università di Bologna, via Selmi 2, 40126 Bologna, Italy

Received: July 18, 2001; In Final Form: January 8, 2002

The binuclear complexes  $[(bpy)_2Ru(\mu-2,3-dpp)Ru(bpy)_2]^{4+}$ ,  $[(bpy)_2Ru(\mu-2,5-dpp)Ru(bpy)_2]^{4+}$ ,  $[(bpy)_2Ru(\mu-2,3-dpp)Os(bpy)_2]^{4+}$ ,  $[(bpy)_2Ru(\mu-2,5-dpp)Os(bpy)_2]^{4+}$ , and  $[(bpy)_2Os(\mu-2,3-dpp)Os(bpy)_2]^{4+}$  (dpp = bis(2-pyridyl)pyrazine, bpy = 2,2-bipyridine, biq = 2,2-biquinoline) have been studied with femtosecond pump–probe spectroscopy. Excitation energy transfer from the Ru to the Os center in the heterometallic binuclear complexes occurs within 200 fs. This is a time scale comparable to the singlet–triplet conversion and vibrational relaxation of the lowest metal-to-ligand charge transfer (MLCT) state in this type of complexes. Thus, energy transfer probably involves nonthermalized initial states, which may be an explanation for the fast transfer rate. Small spectral changes with time constants of ca. 400–800 fs were observed for all complexes examined, and are attributed to relaxation (vibrational and/or spin) of the MLCT state localized on the lowest energy unit. Energy transfer seems to occur within 200 fs also in the symmetric  $Ru^{II}$ – $Ru^{II}$  and  $Os^{II}$ – $Os^{II}$  complexes, although the reaction driving force is zero. The results suggest that very large antennas or photonic wires could be constructed based on these metal complexes, in which energy transfer can occur in several steps over long distances, with only very small losses.

## Introduction

In natural photosynthesis the sunlight is absorbed by several antenna systems, and the excitation energy is efficiently transferred between many chlorophyll molecules before it reaches the reaction center where charge separation occurs.<sup>1</sup> Different kinds of artificial systems have been constructed to mimic photosynthetic light harvesting. Antennas based on porphyrins<sup>2</sup> or smaller organic molecules<sup>3</sup> have been reported. In contrast to systems based on small organic units, which absorbs only in the UV, artificial antennas constructed of transition metal complexes of, e.g., ruthenium and osmium can reach a high absorbance over a large part of the visible spectrum.<sup>4</sup> Some of us have synthesized and studied dendritic structures (see, e.g., Figure 1) with up to as many as 22 ruthenium and/or osmium centers that absorb light over a wide spectral range.<sup>5</sup> By varying the metal, the bridging ligand, and peripheral ligands, it is possible to tune the excited-state energy of each metal complex unit in the dendrimer. The excitation energy is transferred between the units in different patterns depending on their relative excited-state energies.<sup>6</sup> In most cases the emission spectra only display the characteristics of the lowest excited state, irrespective of which metal center is excited, showing that energy transfer is  $\approx 100\%$  efficient. However, the rate of energy transfer between two neighboring metal centers is not known, as the emission spectra only suggest a lower limit of  $k_{EnT} = 1 \times 10^9 \text{ s}^{-1}$ . There is currently a strong interest in

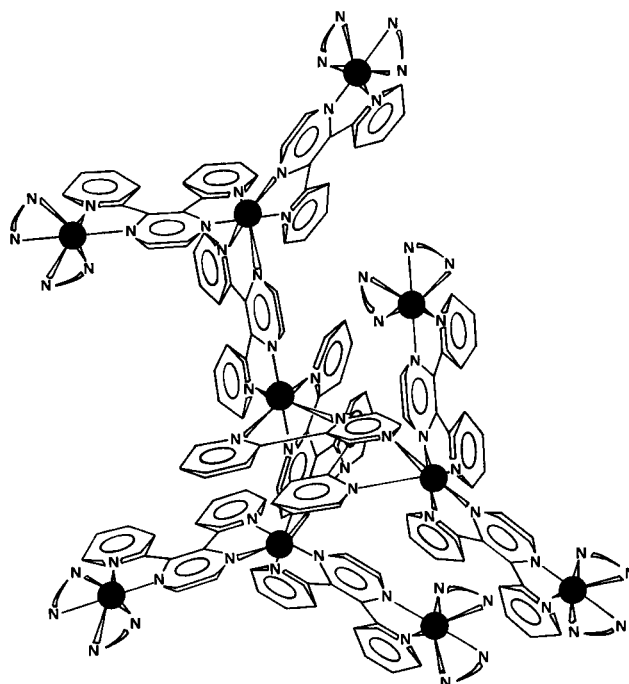


**Figure 1.** Schematic picture of a decanuclear complex. N–N stands for bpy or biq.

the excited-state dynamics of ruthenium complexes, both as separate complexes<sup>7</sup> and in larger assemblies.<sup>8</sup> In addition to being of fundamental interest, the exact rate of energy transfer between neighboring metal centers is of great importance for the overall efficiency of a multistep transfer process, in antennas

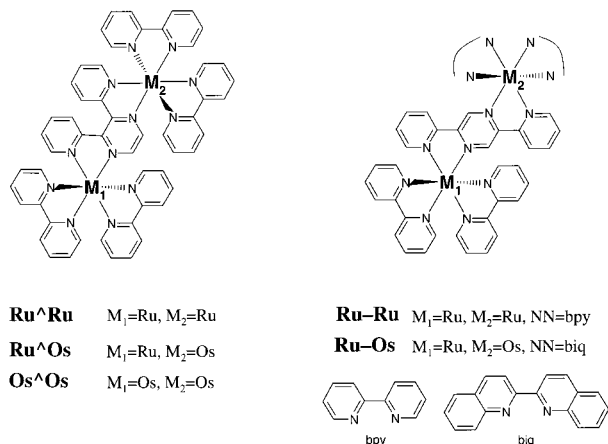
\* Corresponding author. E-mail: Leifh@fki.uu.se.

<sup>†</sup> Uppsala University.

<sup>‡</sup> Università di Messina.

<sup>§</sup> Università di Bologna.

**SCHEME 1: Structure of the Binuclear Complexes: Metal Complexes with (left) 2,3-dpp and (right) 2,5-dpp as Bridging Ligand**



and other photonic devices, since energy transfer competes with intrinsic excited-state decay of each unit ( $\tau \approx 100$  ns).

In the present paper we have examined the excited-state dynamics in binuclear complexes that are models for two neighboring units in antennas of the type exemplified in Figure 1. We present results from pump–probe measurements on two types of dinuclear ruthenium–osmium complexes, differing in the geometry of the bridging ligand (Scheme 1). For comparison, some of the ruthenium–ruthenium and osmium–osmium complexes have also been examined. Thus, the binuclear complexes  $[(\text{bpy})_2\text{Ru}(\mu\text{-}2,3\text{-dpp})\text{Ru}(\text{bpy})_2]^{4+}$ ,  $[(\text{bpy})_2\text{Ru}(\mu\text{-}2,5\text{-dpp})\text{Ru}(\text{bpy})_2]^{4+}$ ,  $[(\text{bpy})_2\text{Ru}(\mu\text{-}2,3\text{-dpp})\text{Os}(\text{bpy})_2]^{4+}$ ,  $[(\text{bpy})_2\text{Ru}(\mu\text{-}2,5\text{-dpp})\text{Os}(\text{biq})_2]^{4+}$ , and  $[(\text{bpy})_2\text{Os}(\mu\text{-}2,3\text{-dpp})\text{Os}(\text{bpy})_2]^{4+}$  (dpp = 2,3- or 2,5-bis(2-pyridyl)pyrazine, bpy = 2,2-bipyridine, biq = 2,2-biquinoline) have been studied. The structures are shown in Scheme 1. The bridging ligands used provide good electronic communication in redox processes<sup>9</sup> so that energy transfer is expected to be rapid.

### Experimental Section

The synthesis of the dinuclear metal complexes and their absorption, emission, and redox properties have been described in detail previously.<sup>9,10</sup> All measurements were performed in acetonitrile of spectroscopic grade at 298 K. Steady state absorption spectra were recorded with a Hewlett-Packard HP 8453 spectrometer. The transient absorption pump–probe measurements were performed with a femtosecond laser system which has been described in detail elsewhere.<sup>11</sup> The pump light was generated in an optical parametric amplifier (TOPAS), and the temporal width of the pulses was 150 fs (800 nm light, autocorrelation half width of 190–200 fs) at a frequency of 1 kHz. A white light continuum, generated in a sapphire window or in water, was used for probing. The probe light was passed through an optical delay line before it was focused and overlapped with the pump light in the  $1 \times 10$  mm sample cell that was continuously moved vertically. In the spectral measurements a spectrograph (MS257, Oriel instruments) equipped with a CCD detector was used. The spectral chirp was  $\approx 1$  ps over the region corresponding to the bleaching of the ground state absorption band. The absorbance at the excitation wavelength was  $\approx 0.3$  in all measurements, and the intensity of the pump pulses was below  $4 \mu\text{J}$ . In the polarization-dependent measurements a polarizer was placed in the pump beam and in the probe beam, respectively. A  $\lambda_{1/2}$  plate was positioned before the white light generation in the probe beam to rotate the fundamental laser

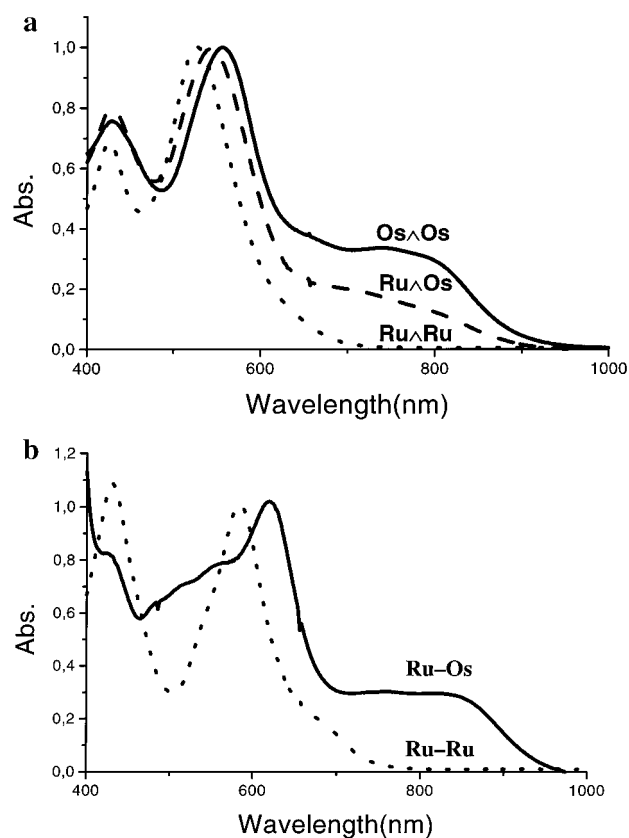


**Figure 2.** (a) Normalized absorption spectra for the complexes with 2,3-dpp as bridging ligand; **Os<sup>^</sup>Os**, **Ru<sup>^</sup>Os**, and **Ru<sup>^</sup>Ru**. (b) Normalized absorption spectra for the complexes with 2,5-dpp as bridging ligand; **Ru–Os** and **Ru–Ru**. Solvent: acetonitrile.

light  $50^\circ$  to generate intensity both parallel and perpendicular to the pump beam. The polarizer in the probe beam was positioned just before the sample and adjusted to select the direction either parallel or perpendicular to excitation.

### Results

**Absorption Spectra.** The absorption spectra of the complexes are shown in Figure 2. The bands in the UV region are due to ligand-centered (LC) transitions (not shown in Figure 2), and the bands in the visible region correspond to metal-to-ligand charge transfer (<sup>1</sup>MLCT) transitions.<sup>12</sup> The energies of the different MLCT transitions depend on the metal from which the electron is transferred as well as on the ligand that accepts the electron. The energy ordering of the MLCT transitions is as follows:  $\text{Os} \rightarrow 2,5\text{-dpp} < \text{Os} \rightarrow 2,3\text{-dpp} < \text{Os} \rightarrow \text{biq} < \text{Ru} \rightarrow 2,5\text{-dpp} < \text{Ru} \rightarrow 2,3\text{-dpp} < \text{Os} \rightarrow \text{bpy} < \text{Ru} \rightarrow \text{bpy}$ .<sup>6</sup> The neighboring ligands, which are coordinated to the same metal, affect the energy of the transition through their effect on the metal. A more electron donating neighbor will lower the energy of the transition. To a smaller extent, the excitation energy of one unit is affected by changing the neighboring *metal* between ruthenium and osmium.<sup>6</sup> On the basis of these considerations, it is possible to determine the relative excited-state energies of the different metal complex units in the antennas.

**Complexes Bridged by 2,3-dpp.** Figure 2a displays absorption spectra for the complexes with 2,3-dpp as bridging ligand. In **Ru<sup>^</sup>Ru** there are two MLCT bands in the visible region:  $\text{Ru} \rightarrow \text{bpy}$  with maximum at 425 nm and  $\text{Ru} \rightarrow 2,3\text{-dpp}$  with maximum at 528 nm.<sup>6</sup> In **Os<sup>^</sup>Os** the  $\text{Os} \rightarrow \text{bpy}$  band is only slightly red shifted, compared to the  $\text{Ru} \rightarrow \text{bpy}$  band in **Ru<sup>^</sup>Ru**, giving a maximum at 428 nm, while the  $\text{Os} \rightarrow 2,3\text{-dpp}$  band is

shifted to 556 nm. In the heteronuclear complex **Ru** $\wedge$ **Os**, the Ru $\rightarrow$ bpy and Os $\rightarrow$ bpy transitions give an absorbance with maximum at 428 nm, while the overlapping Ru $\rightarrow$ 2,3-dpp and Os $\rightarrow$ 2,3-dpp transitions give an absorption with maximum at 544 nm, intermediate between the maxima for **Ru** $\wedge$ **Ru** and **Os** $\wedge$ **Os**. In the compounds containing Os there are additional absorption bands in the red part of the spectrum (700–800 nm). This is due to the direct transitions to the spin-forbidden triplet MLCT states of the Os moiety, which become weakly allowed due to the enhanced spin–orbit coupling.<sup>6,12</sup>

**Complexes Bridged by 2,5-dpp.** In the absorption spectrum for **Ru**–**Ru** (Figure 2b), the MLCT Ru $\rightarrow$ bpy with maximum at 430 nm is red shifted by a few nanometers compared to the corresponding band in **Ru** $\wedge$ **Ru**. The Ru $\rightarrow$ 2,5-dpp transition has a maximum at 575 nm, and is red shifted compared to the corresponding transition in **Ru** $\wedge$ **Ru**. In the absorption spectrum of **Ru**–**Os** new features appear which are due to the Os $\rightarrow$ 2,5-dpp and Os $\rightarrow$ bq transitions as well as transitions to the spin-forbidden triplet MLCT states of the osmium moiety above 700 nm. The Ru $\rightarrow$ bpy and Ru $\rightarrow$ 2,5-dpp bands are expected to be at approximately the same energy as in **Ru**–**Ru**, in analogy with the 2,3-dpp series.<sup>10b</sup> The MLCT transitions of the Os moiety, Os $\rightarrow$ 2,5-dpp, and Os $\rightarrow$ bq overlap to give an absorbance maximum at 610 nm. Since the Os $\rightarrow$ bq band is much red shifted compared to the Ru $\rightarrow$ bpy band, the possibility of selectively exciting the ruthenium moiety in **Ru**–**Os** is better than that in **Ru** $\wedge$ **Os**, if excitation is performed in the Ru $\rightarrow$ bpy band.

**Absorption Spectra of the Oxidized Ru–Os Complexes.** The complexes **Ru** $\wedge$ **Os** and **Ru**–**Os** were oxidized by titration with a Ce(IV) solution. Since Os(II) is 0.4–0.6 V easier to oxidize than Ru(II) in these complexes,<sup>9</sup> the mixed-valence Ru(II)–Os(III) complexes are initially formed. We investigated the spectral changes during titration to support the assignment of the visible bands to overlapping but localized Ru $\rightarrow$ ligand and Os $\rightarrow$ ligand transitions, as opposed to delocalized Ru/Os $\rightarrow$ ligand transitions. As up to 1 equiv of Ce(IV) is added, a band grows in around ca. 1050 nm ( $\epsilon \approx 1 \times 10^3 \text{ M}^{-1} \text{ cm}^{-1}$ ) for **Ru** $\wedge$ **Os** (Figure 3a, inset), which can be attributed to Ru(II) $\rightarrow$ Os(III) intervalence charge transfer.<sup>13</sup> Upon further addition of Ce(IV) the intervalence band disappears, as also the Ru(II) is oxidized. The corresponding band for **Ru**–**Os** is much weaker and difficult to resolve (Figure 3b, inset), but a general increase and subsequent decrease of absorption at 1000–1300 nm is induced by titration with Ce(IV). During titration of the two complexes, also the lowest <sup>1</sup>MLCT bands disappear (Figure 3a,b). Initially, as the Os(II) is oxidized, the greatest change is observed on the red side of these bands. Thus, as the Ru(II)–Os(III) species is formed, the band maximum of **Ru** $\wedge$ **Os** shifts from 544 nm to ca. 530 nm, which is close to the 528 nm maximum of **Ru** $\wedge$ **Ru**. This strongly suggests that the ground-state band is indeed composed of individual Ru(II) $\rightarrow$ dpp and Os(II) $\rightarrow$ dpp bands that are overlapping, and that the latter is red-shifted compared to the former. As more Ce(IV) is added to oxidize the Ru(II), also the Ru(II) $\rightarrow$ dpp band disappears. Similar results were obtained for **Ru**–**Os**, but the <sup>1</sup>MLCT band shift was more pronounced: from 610 nm for the original complex to ca. 575 nm for the Ru(II)–Os(III) species, which is in good agreement with the band maximum for **Ru**–**Ru**.

**Transient Absorption Measurements.** **Complexes Bridged by 2,3-dpp.** Figure 4 shows the transient absorption spectra for **Ru** $\wedge$ **Ru** and **Ru** $\wedge$ **Os**, after excitation at 520 nm, which is on the blue side of the Ru $\rightarrow$ 2,3-dpp and Os $\rightarrow$ 2,3-dpp bands. Excitation at this wavelength directly populates the lowest

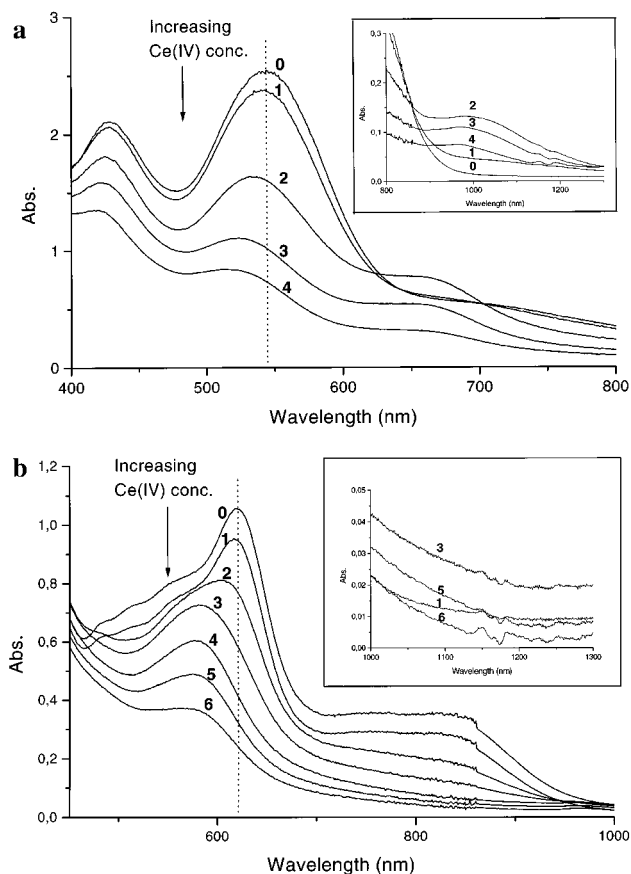


**Figure 3.** Absorption spectra of (a) **Ru** $\wedge$ **Os** and (b) **Ru**–**Os** during titration with a Ce(IV) oxidant. The numbers indicate the order of Ce(IV) additions. The dashed line indicates the wavelength maximum for the main absorption band for the starting Ru(II)–Os(II) state. Insets: the intervalence band of the Ru(II)–Os(III) species first increases and then decreases with increasing Ce(IV) additions, as first the Ru(II)–Os(III) and then the Ru(III)–Os(III) are generated. The maximum Ru(II)–Os(III) concentration is obtained with 1 equiv of Ce(IV) (curve 2 in (a), curve 3 in (b)). For clarity, not all curves were plotted in the inset to (b).

<sup>1</sup>MLCT state in the symmetric complex **Ru** $\wedge$ **Ru**, while the excitation in **Ru** $\wedge$ **Os** is distributed on both the Ru $\rightarrow$ 2,3-dpp and the lower lying Os $\rightarrow$ 2,3-dpp state. Energy transfer from the Ru $\rightarrow$ 2,3-dpp to the Os $\rightarrow$ 2,3-dpp state will then shift the excitation distribution completely to the Os moiety. Immediately after excitation a bleaching of the ground-state absorption is observed for both complexes (Figure 3), due to the relatively small extinction coefficient for the excited state in the visible region. In **Ru** $\wedge$ **Ru** the maximum wavelength of the bleach agrees well with the maximum of the Ru $\rightarrow$ 2,3-dpp band at 528 nm in the ground state absorption spectrum, and there is no spectral shift with time after 3 ps. The excited state has a lifetime of 100 ns<sup>9</sup> and does not decay significantly on the experimental time scale (<1 ns).

In **Ru** $\wedge$ **Os** the Os $\rightarrow$ 2,3-dpp <sup>1</sup>MLCT state is somewhat lower in energy than the corresponding Ru $\rightarrow$ 2,3-dpp state. Excitation at 520 nm, on the blue side of the 544 nm maximum for the overlapping bands, creates the excited Ru $\rightarrow$ 2,3-dpp state in a major fraction of the complexes. When the excitation energy is transferred from the Ru to the Os moiety, a red shift of the transient bleach is expected. However, already after 3 ps, the transient bleach for **Ru** $\wedge$ **Os** is red shifted compared to the ground-state maximum, and corresponds instead to the ground-state maximum of **Os** $\wedge$ **Os**. No further spectral shift with time is seen (Figure 4b). This indicates that the molecule has already

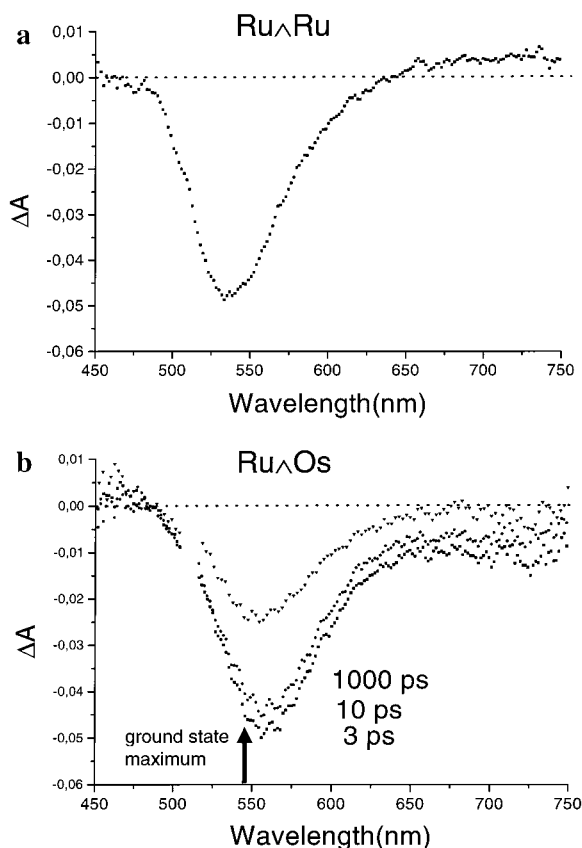


**Figure 4.** Transient absorption spectra of (a)  $\text{Ru}^{\wedge}\text{Ru}$  ( $\Delta t = 1000$  ps; excitation at 512 nm) and (b)  $\text{Ru}^{\wedge}\text{Os}$  ( $\Delta t = 3, 10,$  and  $100$  ps; excitation at 512 nm). The arrow in (b) indicates the position of the ground state absorption maximum (cf. Figure 2a), but the observed bleaching maximum is located at a longer wavelength. Solvent: acetonitrile.

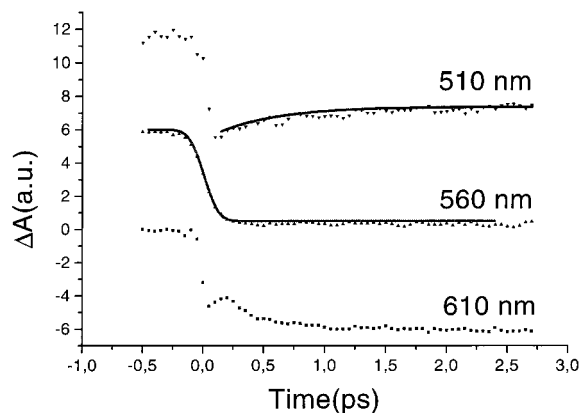


**Figure 5.** Kinetic traces at 510, 560, and 610 nm of  $\text{Ru}^{\wedge}\text{Os}$  after excitation at 520 nm. The solid lines in the 610 and 510 nm traces are single-exponential functions both with a time constant of 400 fs. The line in the 560 nm trace is a simulation of a pulse-limited bleach using a Gaussian cross-correlation function with a half-width of 220 fs.

relaxed to its lowest excited state localized on the osmium moiety, i.e., mainly of  $\text{Os} \rightarrow \text{dpp}$  MLCT character. The decrease in bleaching amplitude with time is due to the decay of the excited  $\text{Os} \rightarrow 2,3\text{-dpp}$  state ( $\tau \approx 1$  ns, based on transient absorption traces), which is much more short-lived than the corresponding  $\text{Ru} \rightarrow 2,3\text{-dpp}$  state in  $\text{Ru}^{\wedge}\text{Ru}$  ( $\tau \approx 100$  ns<sup>9</sup>).

To investigate a possible spectral shift on a shorter time scale than 3 ps, kinetic traces of the bleach at different wavelengths in the spectrum were recorded. Figure 5 shows the result for  $\text{Ru}^{\wedge}\text{Os}$  at probe wavelengths 510, 560, and 610 nm. A pulse-

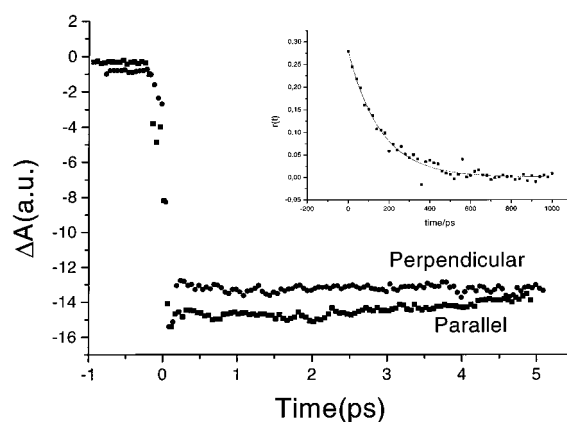


**Figure 6.** Kinetic traces probing at 560 nm parallel and perpendicular to the 550 nm excitation of  $\text{Ru}^{\wedge}\text{Os}$ . The traces are scaled to give similar bleach magnitudes for the purpose of comparison. The inset shows the slow anisotropy decay for  $\text{Ru}^{\wedge}\text{Ru}$  attributed to molecular rotation.

limited bleach<sup>14</sup> is observed at all wavelengths as the ground state is depleted. At the bleach maximum (560 nm) no subsequent change of the signal is seen. At the blue edge (510 nm) instead, a partial recovery of the bleach is seen, while a further bleach is observed at the red edge (610 nm). This corresponds to a spectral red shift of the bleach. A single-exponential fit to the traces gave a time constant of  $\approx 400$  fs for the spectral shift. Excitation energy transfer between the metal moieties in  $\text{Ru}^{\wedge}\text{Ru}$  and  $\text{Os}^{\wedge}\text{Os}$  is not expected to give a spectral shift since these complexes are symmetric. However, after excitation, the kinetic traces at the corresponding wavelengths showed the same shift as for  $\text{Ru}^{\wedge}\text{Os}$ , that is a bleach recovery on the blue side of the spectrum and a further bleaching increase on the red side, both with the same  $\approx 400$  fs time constant as in  $\text{Ru}^{\wedge}\text{Os}$ .

Further experiments were made on the polarization dependence of the pump–probe traces. The transition dipole moment of the lowest MLCT state is directed along the metal–ligand pseudo  $C_{2v}$  axis, which bisects the N–Ru–N angle.<sup>15</sup> Thus, with the bent 2,3-dpp as bridging ligand, energy transfer from one metal unit to the other would change the direction of the transition dipole. This would result in a difference in the kinetic traces when the probe light is perpendicular or parallel to the excitation light. In Figure 6 the result is shown for  $\text{Ru}^{\wedge}\text{Os}$ , where the sample is excited at 550 nm and the bleaching is observed at the 560 nm bleach maximum. There is no difference between the different probe polarizations on the time scale shown ( $< 5$  ps). On longer time scale a slow exponential anisotropy decay, with a lifetime of 150 ps, was observed (Figure 6, inset), presumably due to rotation of the whole complex. In the symmetric complexes,  $\text{Ru}^{\wedge}\text{Ru}$  and  $\text{Os}^{\wedge}\text{Os}$ , the excited states of the two metal centers are equal in energy, but their transition dipole moments have different directions. This would give no spectral shift, but a difference in the bleach magnitude for the kinetic traces with probe light perpendicular and parallel to the excitation as the excitation energy is distributed evenly between the metal centers. However, as for  $\text{Ru}^{\wedge}\text{Os}$ , no anisotropy change was observed for  $\text{Os}^{\wedge}\text{Os}$  and  $\text{Ru}^{\wedge}\text{Ru}$  on a short time scale ( $< 5$  ps),<sup>16</sup> but both complexes exhibit the ca. 150 ps anisotropy decay attributed to molecular rotation.

*Complexes Bridged by 2,5-dpp.* Figure 7 shows the transient absorption spectra for  $\text{Ru}^{\wedge}\text{Ru}$  and  $\text{Ru}^{\wedge}\text{Os}$  after excitation at 513 and 528 nm, respectively. As for  $\text{Ru}^{\wedge}\text{Ru}$ , this directly populates the lowest MLCT state in  $\text{Ru}^{\wedge}\text{Ru}$ , which is  $\text{Ru} \rightarrow 2,5\text{-dpp}$ . In  $\text{Ru}^{\wedge}\text{Os}$  instead, the excitation will be distributed on

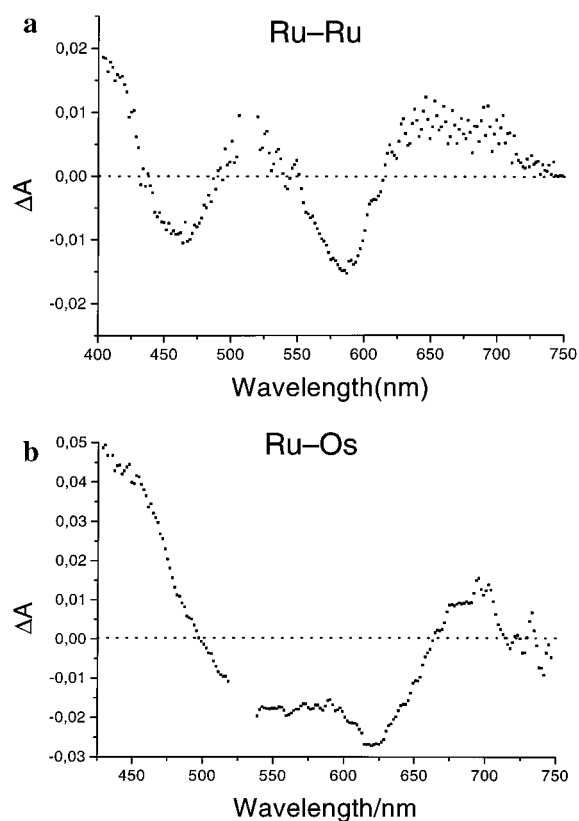


**Figure 7.** Transient absorption spectra of (a) **Ru–Ru** ( $\Delta t = 1000$  ps; excitation at 513 nm) and (b) **Ru–Os** ( $\Delta t = 5$  ps; excitation at 528 nm). Solvent: acetonitrile.

both the  $\text{Ru} \rightarrow 2,5\text{-dpp}$  and the  $\text{Os} \rightarrow 2,5\text{-dpp/biq}$  states. Energy transfer will then shift the excitation distribution completely to the osmium moiety. Excitation of **Ru–Ru** results in an immediate bleach of the  $\text{Ru} \rightarrow \text{bpy}$  and  $\text{Ru} \rightarrow 2,5\text{-dpp}$  transitions (Figure 7), with the maximum of the bands corresponding to those of the ground-state absorption. At 400 nm an increased absorption is seen that can be assigned to transitions of the reduced 2,5-dpp of the MLCT state.<sup>17</sup> The lowest excited state in **Ru–Os** is  $\text{Os} \rightarrow 2,5\text{-dpp}$  or  $\text{Os} \rightarrow \text{biq}$ , but the corresponding absorption bands overlap with the  $\text{Ru} \rightarrow 2,5\text{-dpp}$  band. Excitation at 528 nm, which is on the blue side of the visible absorption maximum, results in a bleaching of the  $\text{Os} \rightarrow 2,5\text{-dpp}$  and  $\text{Os} \rightarrow \text{biq}$  bands already after 5 ps. In contrast, no bleaching of the  $\text{Ru} \rightarrow \text{bpy}$  band is seen at 430 nm. Instead, an absorbance is seen with maximum at 450 nm that can probably be assigned to transitions of the reduced 2,5-dpp<sup>17</sup> or biq<sup>18</sup> of the lowest Os-based MLCT state. No spectral shift is observed at longer times ( $< 1$  ns).

To investigate a possible spectral shift on a time scale shorter than 5 ps in **Ru–Os**, kinetic traces of the transient absorption were recorded at the maximum wavelengths of the absorption bands corresponding to the different MLCT transitions for the Ru and Os moieties. Figure 8 shows kinetic traces at probe wavelengths of 450, 625, and 772 nm after excitation at 555 nm, which is at the blue edge of the  $\text{Ru} \rightarrow 2,5\text{-dpp}$  transition. The result is an immediate absorption at 450 nm (Figure 8a) and an immediate bleach at 625 nm (Figure 8b), without further change of the signals on the time scale shown ( $< 8$  ps). On much longer time scales the transient absorption signals go to zero as the lowest excited state decays to the ground state ( $\tau \approx 1$  ns). On a short time scale the only change of absorption is observed at 772 nm (Figure 8c), where an initial bleach is followed by a small further bleach, with a time constant of  $\approx 800$  fs. At this

wavelength the ruthenium moiety has no ground-state absorption and the bleaching is only due to the osmium-based  $^3\text{MLCT}$  band. The excited **Ru–Ru** instead shows an immediate absorption at 770 nm (not shown), with no further change, attributable to ligand-to-metal charge transfer in analogy with many other excited Ru–polypyridine complexes.<sup>12b</sup> Excitation of **Ru–Os** at 400 nm, which populates the  $\text{Ru} \rightarrow \text{bpy}$  state, shows the same result (not shown) as excitation at 555 nm, with an immediate absorption at 450 nm and an immediate bleach at 625 and 770 nm. Also in this case there was a small further bleach at 770 nm with a time constant of  $\approx 800$  fs. Excitation directly to the spin-forbidden  $^3\text{MLCT}$  states of osmium at 800 nm also gave an immediate bleach at 770 nm, but there was no further bleach on the  $< 8$  ps time scale (Figure 8d).

## Discussion

First we discuss the excited-state properties and previous data that are needed to interpret our transient absorption data and for the discussion of energy transfer. In the following sections we discuss our transient absorption results and the energy transfer mechanism.

**Excited-State Properties.** Excitation of the mononuclear, homoleptic  $\text{Ru}(\text{bpy})_3^{2+}$  complex results in the rapid,<sup>7,19</sup> quantitative<sup>20</sup> formation of a  $^3\text{MLCT}$  state localized on one ligand.<sup>21</sup> When the complex is excited in the visible absorption band, the initially created  $^1\text{MLCT}$  state undergoes a spin change and vibrational relaxation, with all processes presumably occurring on a similar ultrashort time scale. Thus, the relaxed  $^3\text{MLCT}$  state is generated within ca. 300 fs, as judged from transient absorption spectra.<sup>7a</sup> Most data in the literature suggest that the  $^3\text{MLCT}$  state is localized on one ligand, giving formally a  $\text{Ru}(\text{III})(\text{bpy})_2(\text{bpy}\bullet^-)$  state, although the case is less clear concerning the initially created Franck–Condon  $^1\text{MLCT}$  state.<sup>21</sup> A recent study suggested that the initially created  $^1\text{MLCT}$  excited state is delocalized over all ligands and becomes localized with a 60 fs time constant in acetonitrile.<sup>7b</sup> The excitation hops between  $^3\text{MLCT}$  states localized on different ligands on the time scale of tens of picoseconds in acetonitrile.<sup>22</sup> In a complex with different ligands the excitation is clearly localized, as each ligand gives rise to an individual  $\text{Ru} \rightarrow \text{ligand}$  absorption band at an energy that scales linearly with the ligand reduction potential.<sup>23</sup> Due to the rapid interligand hopping, the different  $\text{Ru} \rightarrow \text{ligand}$  states become thermally equilibrated so that emission is normally observed only from the lowest  $\text{Ru} \rightarrow \text{ligand}$  state.<sup>12</sup>

In the binuclear complexes of the present paper, which are bridged by a conjugated dpp ligand, a delocalization of the lowest metal  $\rightarrow$  dpp  $^3\text{MLCT}$  state over both *metal ions* might be conceived. This would imply that there would not be any energy transfer between excited states localized on the different metal units. However, both low-temperature emission<sup>10b</sup> and redox data<sup>10a</sup> for the Ru–Os complexes investigated indicate that the difference in excited-state energy of the MLCT states of the two metal centers (0.4–0.6 eV) is too large to allow for a significant delocalization. Moreover, the properties of the lowest  $^3\text{MLCT}$  state (emission energy and lifetime) for the Ru–Os complexes are very similar to those for the corresponding Os–Os complexes, but very different from the Ru–Ru complexes.<sup>10b</sup> This suggests that the lowest  $^3\text{MLCT}$  state in the Ru–Os is mainly based on the Os moiety. Finally, when **Ru–Ru** is excited in our femtosecond experiments, we observe a net bleaching at 450 nm (Figure 7a) due to bleaching of the  $\text{Ru} \rightarrow \text{bpy}$  band, because the Ru ion is formally oxidized in the lowest excited  $\text{Ru} \rightarrow \text{dpp}$  state. However, no bleaching of the  $\text{Ru} \rightarrow \text{bpy}$  band is

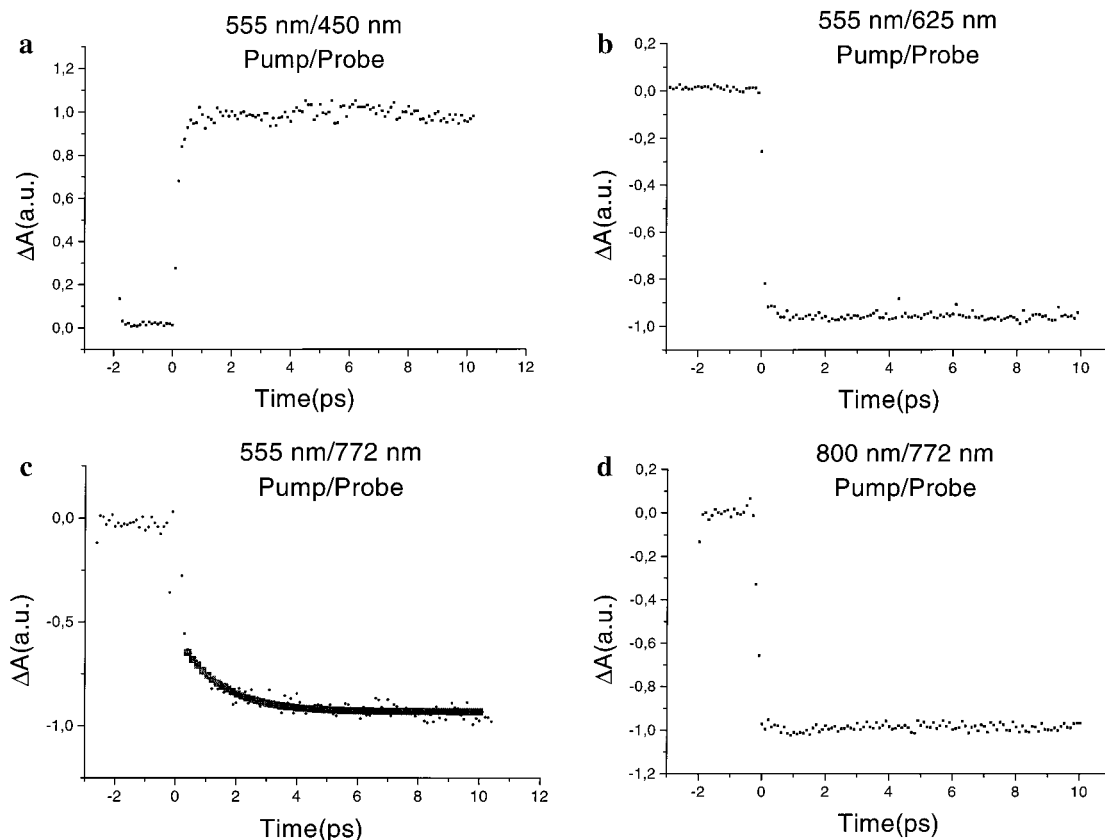


**Figure 8.** Kinetic traces for **Ru–Os** after excitation at 555 nm at probe wavelengths (a) 450, (b) 625, and (c) 770 nm and after excitation at 800 nm at a probe wavelength of (d) 800 nm. The solid line in (c) is a single-exponential function with a time constant of 800 fs.

observed when **Ru–Os** is excited (Figure 7b), but instead a net absorption at 450 nm attributable to the  $\text{dpp}^{\bullet-}$  transitions. The absence of a bleach at 450 nm implies that only the Os metal is oxidized in the lowest excited state of **Ru–Os**, consistent with a  $^3\text{MLCT}$  state localized on only one metal unit. In the transient absorption trace at 450 nm for **Ru–Os** (Figure 8a) the absorption increase is pulse limited, showing that the excited state is localized on the Os unit already on a time scale of  $<200$  fs.

Still, although the thermally equilibrated lowest excited state is a localized  $\text{Os} \rightarrow \text{dpp } ^3\text{MLCT}$  state, it is conceivable that the initially created  $^1\text{MLCT}$  Franck–Condon state could be delocalized, i.e., a  $\text{Ru}/\text{Os} \rightarrow \text{dpp}$  state. If that were the case, then the relaxation to the lowest,  $\text{Os} \rightarrow \text{dpp } ^3\text{MLCT}$  state would rather be described as a localization process than as an energy transfer from the Ru– to the Os moiety. However, this is not consistent with the ground state absorption bands in the visible, which correspond to transitions to the Franck–Condon states. These bands are composed of overlapping bands from localized  $\text{Ru} \rightarrow \text{ligand}$  and  $\text{Os} \rightarrow \text{ligand}$  transitions, where the latter are red shifted compared to the former. In our titration of **Ru $\wedge$ Os** and **Ru–Os** with  $\text{Ce(IV)}$  (Figure 3), during the initial oxidation of  $\text{Os(II)}$  to  $\text{Os(III)}$ , bleaching occurs mainly on the red side of the absorption band that corresponds to the metal  $\rightarrow \text{dpp}$  transitions. The blue side is not bleached as the  $\text{Ru(II)}\text{–Os(III)}$  species is generated, and the resulting band maximum agrees well with the maximum for the corresponding  $\text{Ru(II)}\text{–Ru(II)}$  complexes. This strongly suggests that also the initially prepared Franck–Condon  $^1\text{MLCT}$  states are localized  $\text{Ru} \rightarrow \text{dpp}$  and  $\text{Os} \rightarrow \text{dpp}$  states.

Earlier studies of energy transfer in these complexes have been based on the steady-state emission spectra. The **Ru $\wedge$ Ru** and **Os $\wedge$ Os** complexes display emission maxima at 720 and

928 nm, respectively (at 90 K).<sup>10b</sup> In the heterometallic complex **Ru $\wedge$ Os** the emission spectrum was similar to that of **Os $\wedge$ Os**, with a maximum at 928 nm. Similar results were obtained for **Ru–Os**, in which the only emission observed was from the Os unit, around 900 nm. No Ru-based emission band was seen, indicating an  $\approx 100\%$  efficiency of energy transfer from the Ru to the Os unit. Also, for complexes with a higher nuclearity, such as the family of decanuclear complexes represented in Figure 1, exoergic energy transfer has been shown to occur with an  $\approx 100\%$  efficiency, so that all emission observed at 90 or 298 K originates from the unit with the lowest  $^3\text{MLCT}$  state. With an estimated detection limit of 1% for the Ru-based emission, and an intrinsic lifetime of ca. 100 ns for the Ru excited state, this puts a lower limit of  $1 \times 10^9 \text{ s}^{-1}$  on the energy transfer rate constant. However, with the conjugated dpp bridge of the complexes the rate constant is expected to be much faster than that. For the construction of an efficient artificial antenna in which the excitation energy is transferred rapidly in several steps to one point, without significant losses, the rate constant for each step is important.

**Transient Absorption Results.** Formation of the MLCT states in  $\text{Ru(II)}\text{–}$  and  $\text{Os(II)}\text{–}$  polypyridine complexes leads to the bleaching of the corresponding ground state absorption band, and absorption bands in the visible region that are typically smaller in magnitude.<sup>12</sup> Since the  $\text{Os} \rightarrow \text{dpp}$  absorption bands are red shifted compared to the  $\text{Ru} \rightarrow \text{bpy}$  bands in the present binuclear complexes, the excitation energy transfer from the Ru to the Os center that would result is a red shift of the bleach maximum. However, all our data suggest that the excited-state distribution is localized on the Os center already at the end of our excitation pulses. The transient spectra of **Ru $\wedge$ Os** and **Ru–Os** after a few picoseconds show bleach features with maxima at wavelengths corresponding to the  $\text{Os} \rightarrow \text{dpp}$  ground-

state absorption, and there is no spectral shift at longer times. On a shorter time scale, a small spectral red shift is observed in the kinetic traces of Figures 5 and 8, with time constants of  $\approx 400$  and  $\approx 800$  fs for the complexes bridged by 2,3-dpp and 2,5-dpp, respectively. Since the same shift was observed also in the symmetric Ru–Ru and Os–Os complexes, it cannot be attributed to Ru→Os energy transfer.

Furthermore, there was no polarization dependence in the traces on a  $< 8$  ps time scale. For the complexes bridged by 2,3-dpp, the transition dipole moments of the lowest MLCT state of the two metal centers have different directions, so that an energy transfer is expected to give a polarization dependence of the transient absorption traces for **Ru**∧**Os** as well as for the symmetric **Ru**∧**Ru** and **Os**∧**Os**. Also, this suggests that the  $\approx 400$  fs dynamics observed is not due to energy transfer, but that energy transfer is faster than our time resolution.

For the complexes bridged by 2,5-dpp, the lowest energy Ru→dpp and Os→dpp transition dipole moments are expected to be antiparallel, due to the geometry of the bridge, so that energy transfer cannot be expected to give a polarization dependence of the traces. However, the results from different pump–probe combinations further support our conclusion that energy transfer is faster than the experimental time scale also in **Ru**–**Os**. First, the transient spectra after 5 ps (Figure 7) show a bleach of the Ru→bpy band at 450 nm in **Ru**–**Ru**, while the corresponding spectrum for **Ru**–**Os** shows only the underlying excited-state absorption assigned to the reduced dpp. On a shorter time scale, the kinetic traces at 450 nm after 555 nm excitation (Figure 8a) show a bleach for **Ru**–**Ru** immediately after the excitation pulse, but an immediate positive absorption for **Ru**–**Os**. Thus, the Ru center in **Ru**–**Os** does not seem to be excited on the  $> 200$  fs time scale, consistent with an ultrafast energy transfer. Second, there was an immediate bleach at the maximum for the lowest <sup>1</sup>MLCT transition at 625 nm for **Ru**–**Os**, with no further changes on a  $< 8$  ps time scale (Figure 8b), indicating a complete shift of the excitation to the Os center already at the end of the excitation pulse. Third, the kinetic traces at 770 nm, a wavelength where the only ground-state absorption comes from the Os-based <sup>3</sup>MLCT transitions, an immediate bleach is observed, followed by a further bleach with a time constant of  $800 \pm 200$  fs with a relatively small amplitude (ca. 20% of the total bleach). In contrast, the excited **Ru**–**Ru** gives a small absorption increase at this wavelength, attributable to LMCT transitions in the excited state.<sup>12b</sup> Since excitation at 555 nm will generate at least 50% Ru-based excited states, the 20% amplitude of the 800 fs bleach component is too small to be explained by energy transfer. Thus we conclude that the excitation energy transfer between the metal centers of the complexes investigated must occur on a time scale below our time resolution, i.e.,  $\tau_{\text{EnT}} < 200$  fs!

Instead, we attribute the rapid dynamics observed— $\tau \approx 400$  fs and  $t \approx 800$  fs in the complexes bridged by 2,3-dpp and 2,5-dpp, respectively—to vibrational relaxation, in analogy with observations for the smaller, mononuclear complex  $\text{Ru}(\text{bpy})_3^{2+}$  (see above). Note that excited state absorption bands are present throughout the visible region in this type of complexes.<sup>7,12</sup> Thus, the observed evolution of the bleach signals may be due to a shift of underlying excited-state absorptions that reflect dynamics on the potential surface of the excited state rather than that of the ground state. For **Ru**–**Os**, we followed this dynamics at 770 nm using different excitation wavelengths. Identical results are obtained when exciting at 400 or 555 nm, but with excitation at 800 nm, in the red end of the <sup>3</sup>MLCT band that is probed, only the immediate bleach is observed, with no subsequent

dynamics (Figure 8d). This behavior is consistent with vibrational relaxation, as 800 nm excitation would populate the lowest <sup>3</sup>MLCT state at conformations close to the energy minimum of the potential surface.

**Energy Transfer Mechanism.** The energy transfer seems to occur on the same ultrashort time scale as excited-state relaxation in  $\text{Ru}(\text{bpy})_3^{2+}$  ( $\tau \sim 100$  fs, see above). In contrast to the case in  $\text{Ru}(\text{bpy})_3^{2+}$ , however, also the initial excitation on the Ru center in the present complexes is most likely localized on either the bpy or the dpp ligands since the energies of the Ru→bpy and Ru→dpp excited states are very different, and the corresponding bands are seen in the absorption spectra. However, one can expect that the singlet–triplet and vibrational relaxation occur on a time scale similar to that in  $\text{Ru}(\text{bpy})_3^{2+}$ , which is believed to be complete after 300 fs.<sup>7a</sup> Therefore, we suggest that Ru→Os energy transfer occurs from a nonthermalized excited state, possibly also from the initially populated singlet state(s). Since the MLCT transitions are not very strong in these complexes, not even for the singlet–singlet transitions, a dipole–dipole (Förster-type) mechanism seems unable to account for the very rapid rates inferred. The energy transfer from an initially populated singlet or triplet (thermalized or nonthermalized) Ru→dpp state to the Os→dpp state involving the same bridging ligand can be written as  $(\text{bpy})_2\text{Ru}(\text{III})(\text{dpp}^{\bullet-})\text{Os}(\text{II})(\text{bpy}/\text{biq})_2 \rightarrow (\text{bpy})_2\text{Ru}(\text{II})(\text{dpp}^{\bullet-})\text{Os}(\text{III})(\text{bpy}/\text{biq})_2$ , using the conventional formal notation. However, the notation is misleading in this case, since the reaction is *not* equivalent to a single *electron* transfer from Os(II) to Ru(III). The electron distribution on the dpp ligand is most likely shifted toward the metal involved in the excited state, which is formally oxidized.<sup>10b</sup> In addition, the fractional charge transfer in the MLCT state is somewhat less than 1. Instead, the energy transfer presumably follows an exchange mechanism, but since the reaction may occur from nonthermalized states it can be much more rapid than what might be estimated from conventional models. Thus, even for the symmetric complexes **Ru**∧**Ru** and **Os**∧**Os**, where  $\Delta G^\circ = 0$  and a significant activation energy is predicted if the reactants were thermally equilibrated, energy transfer appears to occur on the time scale of vibrational relaxation.

Interestingly, with 400 nm excitation of **Ru**–**Os**, on the blue side of the Ru→bpy MLCT band, our results were not different from those using lower energy excitation. This shows that the excitation shifts on the  $< 200$  fs time scale from the initially populated Ru→bpy state, which is remote from the Os center, to the Os→dpp state, possibly via the Ru→dpp state. Interligand hopping in the thermalized excited state of  $\text{Ru}(\text{bpy})_3^{2+}$  is much slower ( $\tau \approx 47$  ps in acetonitrile<sup>22</sup>). The faster dynamics observed here may be explained by the fact that the Ru→bpy to Ru→dpp hopping is exoergonic. However, it may also be important that the states are not thermalized, and that the reaction may even involve the singlet MLCT states. This may be very important also for antennas with a higher nuclearity, with a stepwise energy between several metal centers. On an intermediate metal center, the excitation must hop from a Ru→dpp on one side to a Ru→dpp involving another bridging dpp, i.e., an interligand hopping process for which  $\Delta G^\circ \approx 0$ . From the data for  $\text{Ru}(\text{bpy})_3^{2+}$  above, one would predict that this occurs relatively slowly, on a time scale of tens of picoseconds. However, inter-ligand hopping from non-thermalized states can be much faster. Thus, it is possible that also in an energy transfer cascade involving several metal centers, excitation transfer can occur on the  $< 200$  fs time scale. This is important for the construction of larger antennas, photonic wires, and other molecular devices where a rapid energy transfer is desired over

a large distance, with a high yield. A very rapid energy transfer in each step can compete efficiently with other excited state deactivation pathways, and result in small losses of excitation also in multi-step systems. In the present complexes, the lowest <sup>3</sup>MLCT state in **Ru<sup>II</sup>Ru<sup>II</sup>** and **Ru–Ru** has a lifetime of ca. 100 ns. If this represents the intrinsic lifetime of the Ru-based <sup>3</sup>MLCT state on the Ru–Os complexes, energy transfer to the Os center is at least  $5 \times 10^5$  times faster, suggesting that the probability of excitation loss is only  $2 \times 10^{-6}$  in each step.

## Conclusion

Excitation energy transfer from the Ru to the Os center in the dpp-bridged binuclear complexes **Ru<sup>II</sup>Os<sup>II</sup>** and **Ru–Os** occurs within 200 fs. This is a time scale comparable to the singlet–triplet conversion and vibrational relaxation of the lowest MLCT state in this type of complexes. Thus, energy transfer probably involves nonthermalized initial states, which may be an explanation for the fast transfer rate. Small spectral changes with time constants of ca. 400–800 fs were observed in both homo- and heterometallic complexes, and are attributed to vibrational and/or spin relaxation in the lowest excited state. Also, in the symmetric **Ru<sup>II</sup>Ru<sup>II</sup>** and **Os<sup>II</sup>Os<sup>II</sup>** complexes energy transfer seemed to occur within 200 fs. The results suggest that very large antennas or photonic wires could be constructed based on these metal complexes, using the “complexes-as-ligands/complexes-as-metals” strategy,<sup>4a</sup> in which energy transfer can occur in several steps over large distances, with only very small losses.

**Acknowledgment.** This work was supported by the European Commission (TMR Network Contract No. CT96-0031), the Wallenberg Foundation, the Swedish National Energy Administration, the Swedish Research Council for Engineering Sciences (TFR), and the Italian MURST.

## References and Notes

- (1) *The Photosynthetic Reaction Center*; Deisenhofer, J., Norris, J. R., Eds.; Academic Press: San Diego, 1993; Vol. 1-2.
- (2) (a) Lin, V. S.-Y.; DiMaggio, G.; Therien, M. *J. Science* **1994**, *264*, 1105. (b) Kuciauskas, D.; Liddell, P. A.; Lin, S.; Johnson, T. E.; Weghorn, S. J.; Lindsey, J. S.; Moore, A. L.; Moore, T. A.; Gust, D. *J. Am. Chem. Soc.* **1999**, *121*, 8604.
- (3) (a) Shortreed, M. R.; Swallen, S. F.; Shi, Z.-Y.; Tan, W.; Xu, Z.; Devadoss, C.; Moore, J. S.; Kopelman, R. *J. Phys. Chem. B* **1997**, *101*, 6318. (b) Webber, S. E. *Chem. Rev.* **1990**, *90*, 1469. (c) Stewart, G. M.; Fox, M. A. *J. Am. Chem. Soc.* **1996**, *118*, 4354. (d) Devadoss, C.; Bharathi, P.; Moore, J. S. *J. Am. Chem. Soc.* **1996**, *118*, 9635. (e) Gilat, S. L.; Adronov, A.; Fréchet, J. M. J. *Angew. Chem., Int. Ed.* **1999**, *38*, 1422. (f) Adronov, A.; Fréchet, J. M. J. *Chem. Commun.* **2000**, 1701. (g) Neuwahl,

- F. V. R.; Righini, R.; Adronov, A.; Malenfant, P. R. L.; Fréchet, J. M. J. *J. Phys. Chem. B* **2001**, *105*, 1307.
- (4) (a) Balzani, V.; Campagna, S.; Denti, G.; Juris, A.; Serroni, S.; Venturi, M. *Acc. Chem. Res.* **1998**, *31*, 26–34 and references therein. (b) Dupray, L. M.; Devenney, M.; Striplin, D. R.; Meyer, T. J. *J. Am. Chem. Soc.* **1997**, *119*, 10243. (c) Campagna, S.; Serroni, S.; Bodige, S.; MacDonnell, F. M. *Inorg. Chem.* **1999**, *38*, 692. (d) Constable, E. C.; Housecroft, C. E.; Cattalini, M.; Phillips, D. *New J. Chem.* **1998**, *22*, 193. (e) Plevoets, M.; Vogtle, F.; De Cola, L.; Balzani, V. *New J. Chem.* **1999**, *23*, 63. (f) Schultze, X.; Serin, J.; Adronov, A.; Fréchet, J. M. J. *Chem. Commun.* **2001**, 1160.
  - (5) (a) Balzani, V.; Campagna, S.; Denti, G.; Juris, A.; Serroni, S.; Venturi, M. *Acc. Chem. Res.* **1998**, *31*, 26–34 and references therein. (b) Campagna, S.; Denti, G.; Serroni, S.; Juris, A.; Venturi, M.; Ricevuto, V.; Balzani, V. *Chem. Eur. J.* **1995**, *1*, 211. (c) Serroni, S.; Juris, A.; Venturi, M.; Campagna, S.; Resino, I.; Denti, G.; Credi, A.; Balzani, V. *J. Mater. Chem.* **1997**, *7*, 1227–1236.
  - (6) Denti, G.; Campagna, S.; Serroni, S.; Ciano, M.; Balzani, V. *J. Am. Chem. Soc.* **1992**, *114*, 2944–2950.
  - (7) (a) Damrauer, N. H.; Cerullo, G.; Yeh, A.; Boussie, T. R.; Shank, C. V.; McCusker, J. K. *Science* **1997**, *275*, 54. (b) Yeh, A. T.; Shank, C. V.; McCusker, J. K. *Science* **2000**, *289*, 935.
  - (8) (a) Asbury, J. B.; Hao, E.; Wang, Y.; Ghosh, H. N.; Lian, T. J. *J. Phys. Chem. B* **2001**, *105*, 4545. (b) Tachibana, Y.; Haque, S. A.; Mercer, I. P.; Durrant, J. R.; Klug, D. R. *J. Phys. Chem. B* **2000**, *104*, 1198.
  - (9) Denti, G.; Campagna, S.; Sabatino, L.; Serroni, S.; Ciano, M.; Balzani, V. *Inorg. Chem.* **1990**, *29*, 4750–4758.
  - (10) (a) Denti, G.; Serroni, S.; Sabatino, L.; Ciano, M.; Ricevuto, V.; Campagna, S. *Gazz. Chim. Ital.* **1991**, *121*, 37. (b) Juris, A.; Balzani, V.; Campagna, S.; Denti, G.; Serroni, S.; Frei, G.; Güdel, H. *Inorg. Chem.* **1994**, *33*, 1491–1496.
  - (11) Andersson, M.; Davidsson, J.; Hammarström, L.; Korppi-Tommola, J.; Peltola, T. *J. Phys. Chem. B* **1999**, *103*, 3258.
  - (12) (a) Juris, A.; Balzani, V.; Barigelli, F.; Campagna, S.; Belser, P.; von Zelewsky, A. *Coord. Chem. Rev.* **1988**, *84*, 85. (b) Kalyanasundaram, K. In *Photochemistry of Polypyridine and Porphyrin Complexes*; Academic Press: London, 1992.
  - (13) (a) Goldsby, K. A.; Meyer, T. J. *Inorg. Chem.* **1984**, *23*, 3002. (b) Demadis, K. D.; Hartshorn, C. M.; Meyer, T. J. *Chem. Rev.* **2001**, *101*, 2655.
  - (14) The magnitude of the coherence artifacts during the pulse cross-correlation time varied between sample and blanks (solvent). This made deconvolution procedures difficult, and we instead put a conservative upper limit of 200 fs for the energy transfer time constant.
  - (15) Myrick, M. L.; Blakley, R. L.; DeArmond, M. K.; Arthur, M. L. *J. Am. Chem. Soc.* **1988**, *110*, 1325.
  - (16) The anisotropy data for **Ru<sup>II</sup>Ru<sup>II</sup>** have a somewhat lower time resolution than the other experiments, putting a lower time limit of  $\approx 4$  ps for observing anisotropy changes.
  - (17) Balzani, V.; et al. Unpublished results.
  - (18) Meyer, G. Personal communication.
  - (19) Carroll, P. J.; Brus, L. E. *J. Am. Chem. Soc.* **1987**, *109*, 7613.
  - (20) Demas, J. N.; Crosby, G. A. *J. Am. Chem. Soc.* **1971**, *93*, 2841.
  - (21) (a) De Armond, M. K.; Myrick, M. L. *Acc. Chem. Res.* **1989**, *22*, 364. (b) Chen, P.; Meyer, T. J. *Chem. Rev.* **1998**, *98*, 1439.
  - (22) (a) Cooley, L. F.; Bergquist, P.; Kelley, D. F. *J. Am. Chem. Soc.* **1990**, *112*, 2612. (b) Malone, R. A.; Kelley, D. F. *J. Chem. Phys.* **1991**, *95*, 8970.
  - (23) Gorelsky, S. I.; Dodsworth, E. S.; Lever, A. B. P.; Vlcek, A. A. *Coord. Chem. Rev.* **1998**, *174*, 469 and references therein.